Science Advances
AAAS

Supplementary Materials for

Absence of structural brain changes from mindfulness-based stress reduction: Two combined randomized controlled trials

Tammi R. A. Kral, Kaley Davis, Cole Korponay, Matthew J. Hirshberg, Rachel Hoel, Lawrence Y. Tello, Robin I. Goldman, Melissa A. Rosenkranz, Antoine Lutz, Richard J. Davidson*

*Corresponding author. Email: rjdavids@wisc.edu

Published 20 May 2022, *Sci. Adv.* **8**, eabk3316 (2022)
DOI: 10.1126/sciadv.abk3316

This PDF file includes:

Supplementary Text

Multiple Imputation

For intention-to-treat analyses using all assigned participants, we conducted multivariate imputation through chained equations using the MICE package in R (*56*, *57*). We imputed 50 complete datasets using predictive mean matching or logistic regression methods depending on the variable (i.e., continuous or categorical). All variables used in analyses along with baseline scores on anxiety and negative affect were entered into the imputation model as predictors to improve estimation. Due to high correlations between time 1 and time 2 measures of brain structure, we transformed then imputed change score outcomes (i.e., *JAV*; *56*). We confirmed imputation plausibility by plotting the range of imputed values against the range of observed values, the distribution of the imputed values against the distribution of the observed values, and the observed versus imputed values. Convergence was confirmed through plotting the mean and separately the standard deviation of each iteration of imputation for each imputed outcome. We then estimated regression models including all standard covariates for each outcome on each imputed dataset, and pooled results according to Rubin's rules (*58*). Full results are in Tables S4-S5.

Statistical Parametric Mapping (SPM) 12 image processing & analysis

Structural (T1) images were manually realigned to the anterior and posterior commissures (AC-PC), which included adjusting the roll, pitch, and yaw until the AC and PC were in the same axial plane in the sagittal view, and the midlines were oriented vertically in the coronal and axial views. Following manual realignment, T1 images were processed according to the longitudinal pipeline in SPM12 (http://www.fil.ion.ucl.ac.uk/spm). Each participant's Time 1 (baseline) and Time 2 (post-intervention period) scans were then registered using pairwise inverse-consistent alignment in SPM12, including bias field correction, and which generates a subject average (spatial mid-point) image and the Jacobian rate (the difference between the Jacobian determinants for each scan when registered to the mid-point average, divided by the time between scans) (*59*). The average T1 image for each participant was then segmented into gray matter, white matter, and cerebrospinal fluid. The gray matter segmentation of the average T1 from the prior step was then multiplied by the Jacobian rate to give the rate of change in each participant's average space. A study-specific average space was then generated using the DARTEL (Diffeomorphic Anatomical Registration using Exponentiated Lie Algebra) algorithm (*60*), and the participants' T1 images from the prior step aligned and normalized to Montreal Neurological Insitute (MNI) space through the group template. Finally, images were modulated to preserve volume and smoothed with an 8 mm full width at half-maximum (FWHM) Gaussian kernel.

Analysis of rate of change in gray matter density (GMD) from SPM12 was conducted using the SPM12 Estimate function. Wholebrain, voxelwise analysis was conducted using a factorial model with a single, 3-level factor for Group, and covariates to control for participant age, gender, sample, and total gray matter volume. Wholebrain statistical maps for each contrast

(e.g., MBSR-HEP) were corrected using Family-Wise Error (FWE) and thresholded at $p<0.05$. Average GMD rate of change was extracted from each ROI and regressed on Group in a linear model including the same covariates as whole-brain analysis. Analysis of home practice time built from the models of group differences by adding the interaction with home practice time, and thus comparisons were limited to MBSR and HEP. Full results of ROI analysis are in Tables S6-S7.

SPM-Computational Anatomy Toolbox 12 (CAT12) image processing & analysis

The manually realigned T1 images that were used in the SPM12 longitudinal processing pipeline (described above), were additionally processed through the CAT12 longitudinal pipeline that was developed with higher sensitivity to detect smaller changes in brain structure, over relatively shorter periods of time (e.g. scans less than one year apart) compared with the standard SPM12 pipeline (*61*). We used the automated cat_batch_long script, which included modified steps from the standard SPM12 processing pipeline, including tissue segmentation, bias field correction, registration to MNI standard space using the DARTEL algorithm, and modulation to preserve volume. However, while the CAT12 longitudinal pipeline included co-registration of each participants scans, the output from longitudinal processing produced separate files for Time 1 and Time 2, which were entered separately into group analysis. Following the standard CAT12 longitudinal processing, images were smoothed with an 8 mm FWHM Gaussian kernel.

Wholebrain, voxelwise analysis was conducted using a flexible factorial model with 3 factors: Subject, Group, and Time; and the interaction of Group x Time. Participant age, gender, study, and total gray matter volume were included as covariates of no-interest. Contrasts maps were generated for the Group x Time interactions for MBSR versus HEP, and for MBSR versus WL, corrected for multiple comparisons using FWE, and thresholded at $p<0.05$. Average GMD was extracted from each scan (T1 and T2 for each participant, separately) for each ROI using the CAT12 toolbox. ROI analysis was conducted by regressing the GMD differences scores (T2-T1) for each region on Group and including the same covariates as wholebrain analysis. Similar to analysis of SPM12 data, analysis of home practice time built from the models of group differences by adding the interaction with home practice time, and thus comparisons were limited to MBSR and HEP. Full results of ROI analysis are in Table S8-S9.

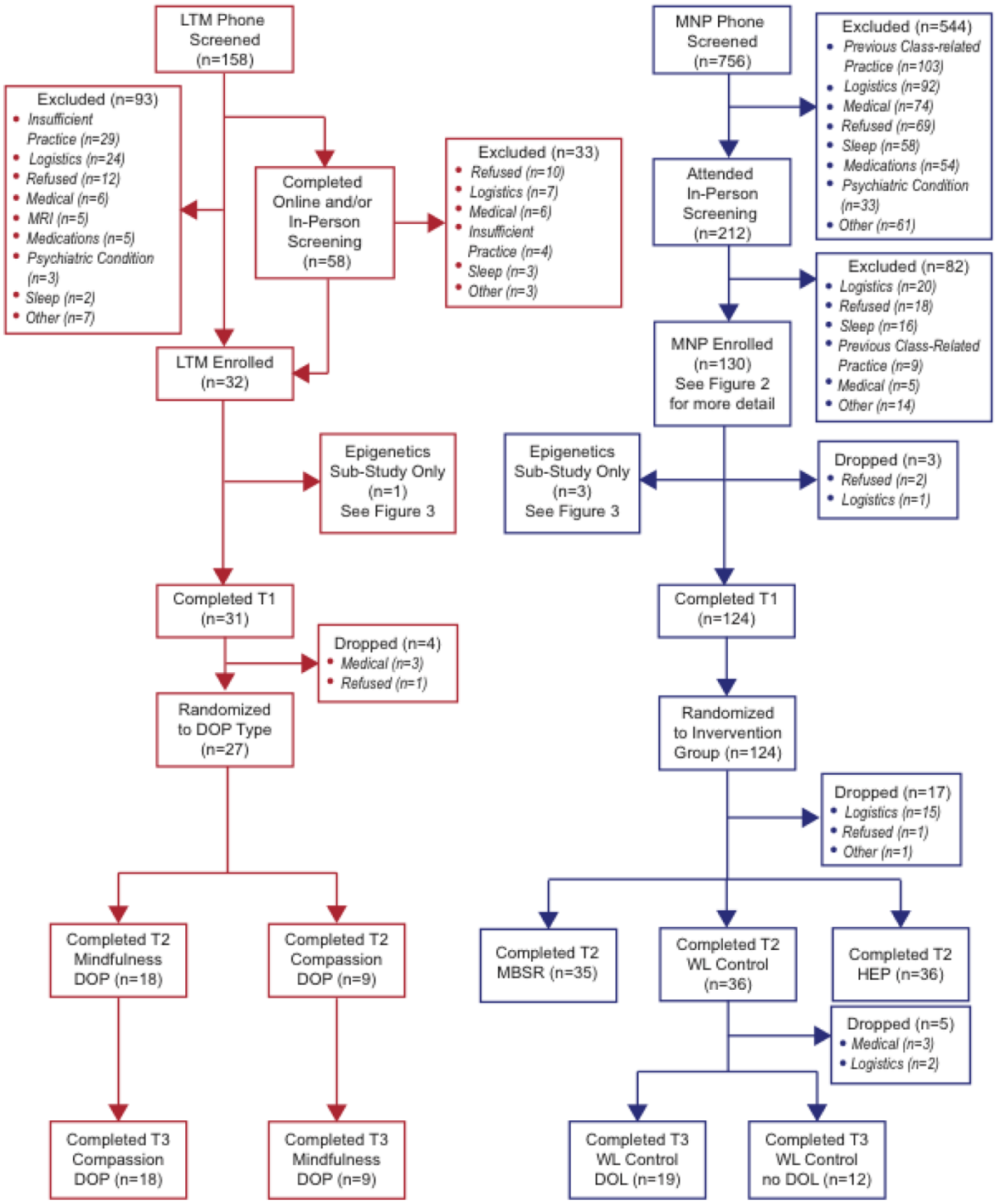

Fig. S1. Dataset 1 CONSORT diagram. This study includes data from the randomized controlled trial of meditation-naïve participants (MNP), shown in blue. Participants completed a baseline visit (T1) prior to randomization to either Mindfulness-Based Stress Reduction (MBSR), the Health Enhancement Program (HEP) active control, or a waitlist control (WL) group. Participants completed a post-intervention (T2) visit, and the WL group also completed a third visit (T3) as a control for the long-term meditators (LTM) in a separate arm of the trial.

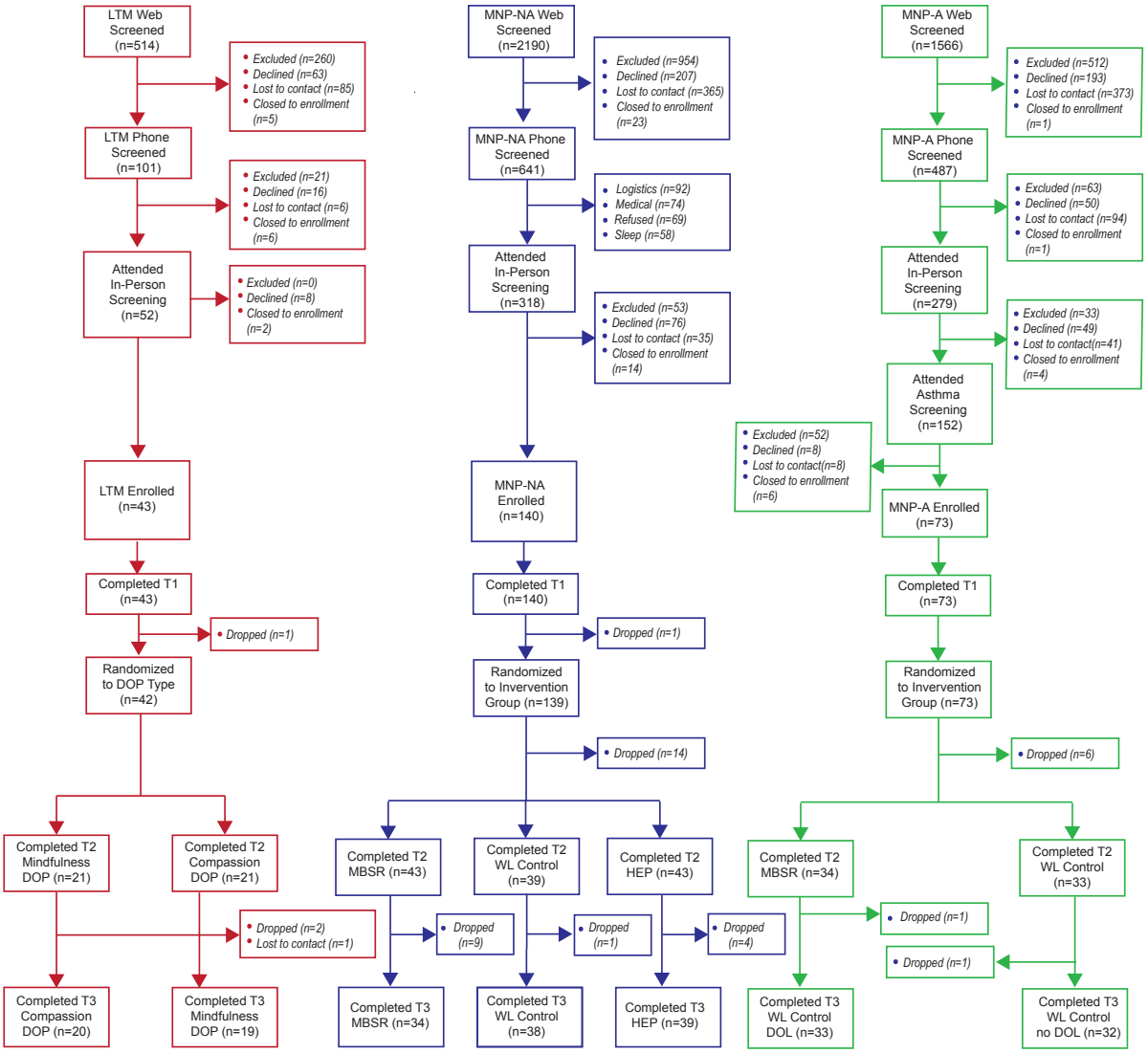

Fig. S2. Dataset 2 CONSORT diagram. This study includes data from the randomized controlled trial of non-asthmatic, meditation-naïve participants (MNP-NA), shown in blue in the middle. Participants completed a baseline lab visit (T1) prior to randomization to either Mindfulness-Based Stress Reduction (MBSR), the Health Enhancement Program (HEP) active control intervention, or a waitlist control (WL) group. Participants completed a post-intervention (T2) lab visit, and a third lab visit for long-term follow-up (T3). Long-term meditators (LTM) and meditation-naïve asthmatics (MNP-A) were not included in the current study, which focused on replicating prior studies on the impact of MBSR.

Table S1.
Within-group changes in brain structure: Cluster details.

Group	Region + Measure	Max.	Peak Coordinates			Size (mm^2)
			X	Y	Z	
MBSR	Left lingual gyrus thickness	4.50	-17	-79	-11	190
HEP	Left rostral middle frontal gyrus thickness	4.32	-22	46	23	143
WL	Left precuneus thickness	4.20	-17	-46	51	155
	Right superior parietal cortex thickness	5.71	18	-61	54	252
	Right precuneus thickness	4.94	9	-55	50	149
	Left rostral middle frontal gyrus volume	4.17	-37	39	27	375

Max = maximum z-value; MBSR = Mindfulness-Based Stress Reduction; HEP = Health Enhancement Program active control; WL = waitlist control

Table S2.
Statistics for analysis of change in regional gray matter volume.

Brain region GMV (mm^3)	Comparison (T2-T1)	Statistic					
		df	*t*	*CI*	pη^2	*p*	*p**
Left amygdala	MBSR vs HEP	198	-1.65	[-31.79:2.84]	0.02	0.10	0.53
	MBSR vs WL	198	-1.40	[-29.54:5.03]	0.02	0.16	0.57
Right amygdala	MBSR vs HEP	198	-0.13	[-19.17:16.88]	<0.01	0.90	0.96
	MBSR vs WL	198	0.38	[-14.83:21.8]	<0.01	0.71	0.77
Left insula	MBSR vs HEP	200	0.05	[-39.79:41.84]	<0.01	0.96	0.96
	MBSR vs WL	200	-0.71	[-56.56:26.72]	<0.01	0.48	0.65
Right insula	MBSR vs HEP	198	0.26	[-40.03:52.40]	0.01	0.79	0.96
	MBSR vs WL	198	-1.19	[-73.95:18.39]	0.01	0.24	0.58
Left caudate	MBSR vs HEP	198	-1.37	[-38.96:7.00]	0.01	0.17	0.53
	MBSR vs WL	198	-0.94	[-34.79:12.32]	0.01	0.35	0.65
Right caudate	MBSR vs HEP	207	0.17	[-19.24:22.84]	0.02	0.87	0.96
	MBSR vs WL	207	1.75	[-2.33:39.91]	0.02	0.08	0.54
Left hippocampus	MBSR vs HEP	201	0.94	[-13.4:37.87]	<0.01	0.35	0.70
	MBSR vs WL	201	0.69	[-16.72:34.76]	<0.01	0.49	0.65
Right hippocampus	MBSR vs HEP	199	2.06	[1.01:47.66]	0.03	0.04	0.48
	MBSR vs WL	199	-0.01	[-23.49:23.18]	0.03	0.99	0.99
Left TPJ	MBSR vs HEP	196	1.32	[-12.46:62.83]	0.01	0.19	0.53
	MBSR vs WL	196	0.70	[-23.94:50.56]	0.01	0.48	0.65
Posterior Cingulate	MBSR vs HEP	198	-1.23	[-103.92:24]	0.01	0.22	0.53
	MBSR vs WL	198	-1.30	[-104.24:21.27]	0.01	0.19	0.57
Cerebellum	MBSR vs HEP	199	-0.47	[-13.58:8.31]	<0.01	0.64	0.96
	MBSR vs WL	199	0.43	[-8.53:13.33]	<0.01	0.67	0.77
Cerebellum/ Brainstem	MBSR vs HEP	204	0.23	[-14.63:18.47]	0.02	0.82	0.96
	MBSR vs WL	204	1.72	[-2.12:31.13]	0.02	0.09	0.54

T2 = post-intervention measure; T1 = baseline/pre-intervention measure; MBSR = Mindfulness-Based Stress Reduction; HEP = Health Enhancement Program active control; WL = waitlist control; GMV = gray matter volume; *df* = degrees of freedom; *CI* = confidence interval; TPJ = temporoparietal junction

Table S3.

Statistics for analysis of MBSR versus HEP practice time and change in GMV (T2-T1).

Brain region (GMV [mm^3]; T2-T1) X Practice (min.) interaction	Statistic					
	df	*t*	*CI*	pη^2	*p*	*p**
Left amygdala: MBSR vs HEP	130	-1.73	[-0.03:0.00]	0.02	0.09	0.26
Right amygdala: MBSR v HEP	**128**	**-3.71**	**[-0.05:-0.01]**	**0.10**	**<0.01**	**<0.01**
MBSR	64	-1.59	[-0.05:-0.01]	0.04	0.12	0.63
HEP	63	0.58	[-0.01:0.01]	0.01	0.57	0.74
Left insula	131	1.82	[0.00:0.06]	0.02	0.07	0.26
Right insula	127	0.66	[-0.03:0.06]	<0.01	0.51	0.68
Left caudate	132	-0.80	[-0.03:0.01]	<0.01	0.43	0.68
Right caudate	136	-0.02	[-0.02:0.01]	<0.01	0.98	0.98
Left hippocampus	132	1.58	[0.00:0.03]	0.02	0.12	0.28
Right hippocampus	131	0.67	[-0.01:0.02]	<0.01	0.50	0.68
Left TPJ	127	0.66	[-0.03:0.05]	<0.01	0.51	0.68
Posterior Cingulate	127	2.13	[0.01:0.14]	0.03	0.04	0.21
Cerebellum	131	-0.39	[-0.01:0.01]	<0.01	0.70	0.83
Brainstem	132	0.18	[-0.01:0.01]	<0.01	0.85	0.93

MBSR = Mindfulness-Based Stress Reduction; HEP = Health Enhancement Program active control; GMV = gray matter volume; T2 = post-intervention measure; T1 = baseline/pre-intervention measure; TPJ = temporo-parietal junction; *df* = degrees of freedom; *CI* = confidence interval

Table S4.

Statistics for analysis of change of regional gray matter volume using multiple imputation.

Brain region GMV (mm^3)	Comparison (T2-T1)	Statistic					
		df	*t*	*CI*	pη^2	*p*	*p**
Left amygdala	MBSR vs HEP	192.21	-1.11	[-32.54, 9.04]	0.01	0.27	0.98
	MBSR vs WL	207.38	-0.74	[-28.64, 13.03]	<0.01	0.46	0.98
Right amygdala	MBSR vs HEP	196.22	0.83	[-12.80, 31.52]	<0.01	0.41	0.98
	MBSR vs WL	201.25	1.07	[-19.34, 34.71]	0.01	0.29	0.98
Left insula	MBSR vs HEP	172.26	-0.32	[-59.35, 42.98]	<0.01	0.75	0.98
	MBSR vs WL	192.53	-0.95	[-75.24, 26.48]	<0.01	0.35	0.98
Right insula	MBSR vs HEP	192.00	1.75	[-6.63, 112.34]	0.02	0.08	0.97
	MBSR vs WL	177.09	-1.12	[-97.35, 27.06]	0.01	0.27	0.98
Left caudate	MBSR vs HEP	184.78	-0.96	[-43.28, 14.94]	0.01	0.34	0.98
	MBSR vs WL	196.97	-0.03	[-29.70, 28.94]	<0.01	0.98	0.98
Right caudate	MBSR vs HEP	215.08	-0.33	[-31.62, 22.50]	<0.01	0.74	0.98
	MBSR vs WL	204.89	0.65	[-18.87, 22.50]	<0.01	0.52	0.98
Left hippocampus	MBSR vs HEP	207.78	0.92	[-15.14, 41.86]	<0.01	0.36	0.98
	MBSR vs WL	192.66	0.68	[-19.57, 40.01]	<0.01	0.50	0.98
Right hippocampus	MBSR vs HEP	201.30	1.77	[-2.69, 49.72]	0.02	0.08	0.97
	MBSR vs WL	204.06	0.42	[-21.10, 32.35]	<0.01	0.68	0.98
Left TPJ	MBSR vs HEP	205.78	0.25	[-48.18, 62.00]	<0.01	0.81	0.98
	MBSR vs WL	210.29	-0.13	[-59.84, 52.25]	<0.01	0.89	0.98
Posterior Cingulate	MBSR vs HEP	204.43	-0.05	[-91.01, 86.31]	<0.01	0.96	0.98
	MBSR vs WL	208.16	-0.43	[-110.08, 70.51]	<0.01	0.67	0.98
Cerebellum	MBSR vs HEP	203.67	-0.94	[-21.54, 7.66]	<0.01	0.92	0.98
	MBSR vs WL	207.93	-0.64	[-19.65, 10.07]	<0.01	0.889	0.98
Cerebellum/ Brainstem	MBSR vs HEP	220.10	-0.94	[-27.35, 9.65]	0.01	0.63	0.98
	MBSR vs WL	230.75	0.15	[-17.20, 20.09]	<0.01	0.62	0.98

T2 = post-intervention measure; T1 = baseline/pre-intervention measure; MBSR = Mindfulness-Based Stress Reduction; HEP = Health Enhancement Program active control; WL = waitlist control; GMV = gray matter volume; *df* = degrees of freedom; *CI* = confidence interval; TPJ = temporoparietal junction

Table S5.
Statistics for MI analysis of MBSR versus HEP practice time and change in GMV.

Brain region (GMV [mm^3]; T2-T1) X Practice (min.) interaction	Statistic					
	df	*t*	*CI*	pη^2	*p*	*p**
Left amygdala	143.03	0.71	[-0.01, 0.02]	0.01	0.478	.637
Right amygdala	143.03	1.89	[-0.001, 0.03]	0.02	0.061	.340
Left insula GMV	143.03	-1.25	[-0.06, 0.01]	0.02	.214	.514
Right insula	143.03	-1.85	[-0.08, .003]	0.02	.066	.340
Left caudate	143.03	0.20	[-0.02, 0.02]	<0.01	.844	.921
Right caudate	143.03	-1.55	[-0.04, 0.005]	0.02	.123	.369
Left hippocampus	143.03	-0.85	[-0.03, 0.01]	0.01	.397	.560
Right hippocampus	143.03	-0.58	[-0.02, 0.01]	0.01	.566	.679
Left TPJ	143.03	0.92	[-0.02, 0.06]	0.01	.359	.560
Posterior Cingulate	143.03	0.04	[-0.11, 0.03]	<0.01	.315	.560
Cerebellum	143.03	1.73	[-0.001. 0.02]	0.03	.085	.340
Brainstem	143.03	-0.004	[-0.01. 0.01]	<0.01	.997	.997

MI = multiple imputation; T2 = post-intervention measure; T1 = baseline/pre-intervention measure; MBSR = Mindfulness-Based Stress Reduction; HEP = Health Enhancement Program active control; GMV = gray matter volume; TPJ = temporo-parietal junction; *df* = degrees of freedom; *CI* = confidence interval

Table S6.
Statistics for analysis of rate of change of regional gray matter density from SPM12.

Brain region (GMD)	Comparison (T2-T1)	Statistic					
		df	*t*	*CI*	pη^2	*p*	*p**
Left amygdala	MBSR vs HEP	198	-0.74	[-5.73:2.59]	<0.01	0.46	0.61
	MBSR vs WL	198	-0.44	[-5.14:3.25]	<0.01	0.6 6	0.94
Right amygdala	MBSR vs HEP	201	-0.24	[-4.91:3.86]	<0.01	0.81	0.83
	MBSR vs WL	201	-0.18	[-4.73:3.94]	<0.01	0.86	0.94
Left insula	MBSR vs HEP	197	-0.57	[-29.12:16.09]	0.01	0.57	0.68
	MBSR vs WL	197	1.11	[-9.86:35.14]	0.01	0.27	0.94
Right insula	MBSR vs HEP	197	-1.97	[-40.53:0.06]	0.02	0.05	0.45
	MBSR vs WL	197	-1.04	[-31.68:9.76]	0.02	0.30	0.94
Left caudate	MBSR vs HEP	201	-1.58	[-18.18:2.02]	0.01	0.12	0.45
	MBSR vs WL	201	-0.28	[-11.75:8.80]	0.01	0.78	0.94
Right caudate	MBSR vs HEP	197	0.21	[-9.15:11.32]	<0.01	0.83	0.83
	MBSR vs WL	197	0.88	[-5.68:14.93]	<0.01	0.38	0.94
Left hippocampus	MBSR vs HEP	200	-1.18	[-16.82:4.22]	0.01	0.24	0.55
	MBSR vs WL	200	-0.05	[-10.93:10.43]	0.01	0.96	0.96
Right hippocampus	MBSR vs HEP	200	0.88	[-5.91:15.45]	<0.01	0.38	0.57
	MBSR vs WL	200	0.31	[-9.11:12.50]	<0.01	0.76	0.94
Left TPJ	MBSR vs HEP	199	-1.46	[-8.08:1.20]	0.02	0.15	0.45
	MBSR vs WL	199	0.49	[-3.62:5.99]	0.02	0.63	0.94
Posterior Cingulate	MBSR vs HEP	200	-1.00	[-5.46:1.79]	0.02	0.32	0.55
	MBSR vs WL	200	0.98	[-1.86:5.55]	0.02	0.33	0.94
Cerebellum	MBSR vs HEP	197	-1.54	[-6.23:0.76]	0.01	0.12	0.45
	MBSR vs WL	197	-0.64	[-4.67:2.39]	0.01	0.52	0.94
Cerebellum/ Brainstem	MBSR vs HEP	195	-1.09	[-7.09:2.05]	0.01	0.28	0.55
	MBSR vs WL	195	0.38	[-3.76:5.53]	0.01	0.71	0.94

SPM = Statistical Parametric Mapping; MBSR = Mindfulness-Based Stress Reduction; HEP = Health Enhancement Program active control; WL = waitlist control; GMD = gray matter density; T2 = post-intervention measure; T1 = baseline/pre-intervention measure; *df* = degrees of freedom; *CI* = confidence interval; TPJ = temporoparietal junction

Table S7.
Statistics for SPM12 analysis of MBSR versus HEP practice time and rate of change in GMD.

Brain region (GMD; T2-T1) X Practice (min.) interaction	Statistic					
	df	*t*	*CI*	pη^2	*p*	*p**
Left amygdala	129	1.12	[0.00:0.01]	0.01	0.26	0.81
Right amygdala	133	-0.21	[0.00:0.00]	<0.01	0.83	0.83
Left insula GMV	130	0.60	[-0.01:0.02]	<0.01	0.55	0.83
Right insula	132	0.95	[-0.01:0.02]	0.01	0.34	0.81
Left caudate	134	-1.01	[-0.01:0.00]	0.01	0.31	0.81
Right caudate	127	1.56	[0.00:0.02]	0.02	0.12	0.73
Left hippocampus	133	2.20	[0.00:0.02]	0.04	0.03	0.36
Right hippocampus	133	0.49	[-0.01:0.01]	<0.01	0.63	0.83
Left TPJ	132	0.25	[0.00:0.00]	<0.01	0.81	0.83
Posterior Cingulate	133	-0.40	[0.00:0.00]	<0.01	0.69	0.83
Cerebellum	129	0.37	[0.00:0.00]	<0.01	0.71	0.83
Brainstem	129	0.84	[0.00:0.01]	0.01	0.40	0.81

SPM = Statistical Parametric Mapping; GMD = gray matter density; MBSR = Mindfulness-Based Stress Reduction; HEP = Health Enhancement Program active control; T2 = post-intervention measure; T1 = baseline/pre-intervention measure; TPJ = temporo-parietal junction; *df* = degrees of freedom; *CI* = confidence interval

Table S8.
Statistics for analysis of change of regional gray matter density from SPM-CAT12.

Brain region GM	Comparison (T2-T1)	Statistic					
		df	*t*	*CI*	pη^2	*p*	*p**
Left amygdala	MBSR vs HEP	198	0.62	[-6.52:12.49]	<0.01	0.54	0.77
	MBSR vs WL	198	0.74	[-6.08:13.33]	<0.01	0.46	0.61
Right amygdala	MBSR vs HEP	198	0.19	[-11.77:14.31]	<0.01	0.85	0.85
	MBSR vs WL	198	0.83	[-7.73:18.90]	<0.01	0.41	0.61
Left insula	MBSR vs HEP	200	1.74	[-5.20:82.08]	0.01	0.08	0.48
	MBSR vs WL	200	0.88	[-24.21:63.60]	0.01	0.38	0.61
Right insula	MBSR vs HEP	203	0.60	[-28.85:53.98]	<0.01	0.55	0.77
	MBSR vs WL	203	0.56	[-30.30:54.14]	<0.01	0.58	0.70
Left caudate	MBSR vs HEP	199	0.38	[-14.29:21.10]	<0.01	0.70	0.77
	MBSR vs WL	199	0.89	[-9.97:26.33]	<0.01	0.37	0.61
Right caudate	MBSR vs HEP	197	-0.93	[-28.12:10.10]	0.02	0.35	0.77
	MBSR vs WL	197	0.80	[-11.41:26.97]	0.02	0.42	0.61
Left hippocampus	MBSR vs HEP	203	-0.79	[-23.67:10.14]	0.01	0.43	0.77
	MBSR vs WL	203	0.37	[-14.00:20.52]	0.01	0.71	0.77
Right hippocampus	MBSR vs HEP	201	0.38	[-12.07:17.81]	<0.01	0.71	0.77
	MBSR vs WL	201	0.77	[-9.16:21.00]	<0.01	0.44	0.61
Left TPJ	MBSR vs HEP	198	1.24	[-1.87:8.16]	0.01	0.22	0.77
	MBSR vs WL	198	0.04	[-5.03:5.24]	0.01	0.97	0.97
Posterior Cingulate	MBSR vs HEP	198	-0.55	[-26.2:14.79]	0.02	0.58	0.77
	MBSR vs WL	198	-1.73	[-38.91:2.56]	0.02	0.09	0.61
Cerebellum	MBSR vs HEP	201	0.47	[-7.50:12.25]	0.02	0.64	0.77
	MBSR vs WL	201	-1.39	[-17.17:2.97]	0.02	0.17	0.61
Cerebellum/ Brainstem	MBSR vs HEP	197	-1.74	[-13.34:0.85]	0.02	0.08	0.48
	MBSR vs WL	197	-1.14	[-11.51:3.05]	0.02	0.25	0.61

SPM-CAT = Statistical Parametric Mapping Computational Anatomy Toolbox; MBSR = Mindfulness-Based Stress Reduction; HEP = Health Enhancement Program active control; WL = waitlist control; GMD = gray matter density; T2 = post-intervention measure; T1 = baseline/pre-intervention measure; *df* = degrees of freedom; *CI* = confidence interval; TPJ = temporoparietal junction

Table S9.
Statistics for SPM-CAT12 analysis of MBSR versus HEP practice time and change in GMD.

Brain region (GMD; T2-T1) X Practice (min.) interaction	Statistic					
	df	*t*	*CI*	pη^2	*p*	*p**
Left amygdala	129	0.29	[-0.01:0.01]	<0.01	0.77	0.98
Right amygdala	**129**	**-2.67**	**[-0.03:0.00]**	**0.05**	**0.01**	**0.10**
Left insula GMV	129	0.95	[-0.02:0.05]	0.01	0.35	0.87
Right insula	132	-0.09	[-0.04:0.03]	<0.01	0.93	0.98
Left caudate	130	-0.14	[-0.01:0.01]	<0.01	0.89	0.98
Right caudate	132	-0.90	[-0.02:0.01]	0.01	0.37	0.87
Left hippocampus	132	-0.02	[-0.01:0.01]	<0.01	0.98	0.98
Right hippocampus	129	-2.03	[-0.02:0.00]	0.03	0.04	0.27
Left TPJ	129	-0.71	[-0.01:0.00]	<0.01	0.48	0.87
Posterior Cingulate	132	0.67	[-0.01:0.02]	<0.01	0.51	0.87
Cerebellum	133	-0.37	[-0.01:0.01]	<0.01	0.71	0.98
Brainstem	132	-0.80	[-0.01:0.00]	<0.01	0.42	0.87

SPM-CAT = Statistical Parametric Mapping Computational Anatomy Toolbox; MBSR = Mindfulness-Based Stress Reduction; HEP = Health Enhancement Program active control; GMD = gray matter density; TPJ = temporo-parietal junction; *df* = degrees of freedom; *CI* = confidence interval

REFERENCES AND NOTES

1. C. Congleton, B. K. Hölzel, S. W. Lazar, *Mindfulness Can Literally Change Your Brain* (Harvard Business Review, 2015).

2. B. Schulte, *Harvard Neuroscientist: Meditation Not Only Reduces Stress, Here's How it Changes Your Brain* (Washington Post, 2015).

3. S. B. Goldberg, R. P. Tucker, P. A. Green, R. J. Davidson, B. E. Wampold, D. J. Kearney, T. L. Simpson, Mindfulness-based interventions for psychiatric disorders: A systematic review and meta-analysis. *Clin. Psychol. Rev.* **59**, 52–60 (2018).

4. J. Kabat-Zinn, An outpatient program in behavioral medicine for chronic pain patients based on the practice of mindfulness meditation: Theoretical considerations and preliminary results. *Gen. Hosp. Psychiatry* **4**, 33–47 (1982).

5. J. Wielgosz, S. B. Goldberg, T. R. A. Kral, J. D. Dunne, R. J. Davidson, Mindfulness meditation and psychopathology. *Annu. Rev. Clin. Psychol.* **15**, 285–316 (2019).

6. A. Chiesa, A. Serretti, Mindfulness-based stress reduction for stress management in healthy people: A review and meta-analysis. *J. Altern. Complement. Med.* **15**, 593–600 (2009).

7. G. Desbordes, L. T. Negi, T. W. W. Pace, B. A. Wallace, C. L. Raison, E. L. Schwartz, Effects of mindful-attention and compassion meditation training on amygdala response to emotional stimuli in an ordinary, non-meditative state. *Front. Hum. Neurosci.* **6**, 292 (2012).

8. T. R. A. Kral, B. S. Schuyler, J. A. Mumford, M. A. Rosenkranz, A. Lutz, R. J. Davidson, Impact of short- and long-term mindfulness meditation training on amygdala reactivity to emotional stimuli. *Neuroimage* **181**, 301–313 (2018).

9. A. Chiesa, R. Calati, A. Serretti, Does mindfulness training improve cognitive abilities? A systematic review of neuropsychological findings. *Clin. Psychol. Rev.* **31**, 449–464 (2011).

10. S. N. Gallant, Mindfulness meditation practice and executive functioning: Breaking down the benefit. *Conscious. Cogn.* **40**, 116–130 (2016).

11. T. Gard, B. K. Hölzel, A. T. Sack, H. Hempel, S. W. Lazar, D. Vaitl, U. Ott, Pain attenuation through mindfulness is associated with decreased cognitive control and increased sensory processing in the brain. *Cereb. Cortex* **22**, 2692–2702 (2012).

12. F. Zeidan, D. R. Vago, Mindfulness meditation–based pain relief: A mechanistic account. *Ann. N. Y. Acad. Sci.* **1373**, 114–127 (2016).

13. K. C. R. Fox, S. Nijeboer, M. L. Dixon, J. L. Floman, M. Ellamil, S. P. Rumak, P. Sedlmeier, K. Christoff, Is meditation associated with altered brain structure? A systematic review and meta-analysis of morphometric neuroimaging in meditation practitioners. *Neurosci. Biobehav. Rev.* **43**, 48–73 (2014).

14. S. J. Colcombe, K. I. Erickson, P. E. Scalf, J. S. Kim, R. Prakash, E. McAuley, S. Elavsky, D. X. Marquez, L. Hu, A. F. Kramer, Aerobic Exercise training increases brain volume in aging humans. *J. Gerontol. A Biol. Sci. Med. Sci.* **61**, 1166–1170 (2006).

15. A. Rogge, B. Röder, A. Zech, K. Hötting, Exercise-induced neuroplasticity: Balance training increases cortical thickness in visual and vestibular cortical regions. *Neuroimage* **179**, 471–479 (2018).

16. R. Ilg, A. M. Wohlschläger, C. Gaser, Y. Liebau, R. Dauner, A. Wöller, C. Zimmer, J. Zihl, M. Mühlau, Gray matter increase induced by practice correlates with task-specific activation: A combined functional and morphometric magnetic resonance imaging study. *J. Neurosci.* **28**, 4210–4215 (2008).

17. B. K. Hölzel, J. Carmody, M. Vangel, C. Congleton, S. M. Yerramsetti, S. W. Lazar, Mindfulness practice leads to increases in regional brain gray matter density. *Psychiatry Res.* **191**, 36–43 (2011).

18. N. A. S. Farb, Z. V. Segal, A. K. Anderson, Mindfulness meditation training alters cortical representations of interoceptive attention. *Soc. Cogn. Affect. Neurosci.* **8**, 15–26 (2013).

19. C.-C. Yang, A. Barrós-Loscertales, M. Li, D. Pinazo, V. Borchardt, C. Ávila, M. Walter, Alterations in brain structure and amplitude of low-frequency after 8 weeks of mindfulness meditation training in meditation-naïve subjects. *Sci. Rep.* **9**, 10977 (2019).

20. N. Kriegeskorte, W. K. Simmons, P. S. Bellgowan, C. I. Baker, Circular analysis in systems neuroscience: The dangers of double dipping. *Nat. Neurosci.* **12**, 535–540 (2009).

21. R. J. Davidson, A. W. Kaszniak, Conceptual and methodological issues in research on mindfulness and meditation. *Am. Psychol.* **70**, 581–592 (2015).

22. J. P. A. Ioannidis, Why most published research findings are false. *PLOS Med.* **2**, e124 (2005).

23. R. Moonesinghe, M. J. Khoury, A. C. J. W. Janssens, Most published research findings are false—But a Little replication goes a long way. *PLOS Med.* **4**, e28 (2007).

24. K. S. Button, J. P. A. Ioannidis, C. Mokrysz, B. A. Nosek, J. Flint, E. S. J. Robinson, M. R. Munafò, Power failure: Why small sample size undermines the reliability of neuroscience. *Nat. Rev. Neurosci.* **14**, 365–376 (2013).

25. R. J. Zatorre, R. D. Fields, H. Johansen-Berg, Plasticity in gray and white: Neuroimaging changes in brain structure during learning. *Nat. Neurosci.* **15**, 528–536 (2012).

26. J. Dewey, G. Hana, T. Russell, J. Price, D. McCaffrey, J. Harezlak, E. Sem, J. C. Anyanwu, C. R. Guttman, B. Navia, R. Cohen, D. F. Tate; HIV Neuroimaging Consortium, Reliability and validity of MRI-based automated volumetry software relative to auto-assisted manual measurement of subcortical structures in HIV-infected patients from a multisite study. *Neuroimage* **51**, 1334–1344 (2010).

27. M. J. Clarkson, M. J. Cardoso, G. R. Ridgway, M. Modat, K. K. Leung, J. D. Rohrer, N. C. Fox, S. Ourselin, A comparison of voxel and surface based cortical thickness estimation methods. *Neuroimage* **57**, 856–865 (2011).

28. A. Lutz, A. P. Jha, J. D. Dunne, C. D. Saron, Investigating the phenomenological matrix of mindfulness-related practices from a neurocognitive perspective. *Am. Psychol.* **70**, 632–658 (2015).

29. W. W. Seeley, V. Menon, A. F. Schatzberg, J. Keller, G. H. Glover, H. Kenna, A. L. Reiss, M. D. Greicius, Dissociable intrinsic connectivity networks for salience processing and executive control. *J. Neurosci.* **27**, 2349–2356 (2007).

30. K. C. R. Fox, R. N. Spreng, M. Ellamil, J. R. Andrews-Hanna, K. Christoff, The wandering brain: Meta-analysis of functional neuroimaging studies of mind-wandering and related spontaneous thought processes. *Neuroimage* **111**, 611–621 (2015).

31. R. N. Spreng, R. A. Mar, A. S. N. Kim, The common neural basis of autobiographical memory, prospection, navigation, theory of mind, and the default mode: A quantitative meta-analysis. *J. Cogn. Neurosci.* **21**, 489–510 (2009).

32. S. Jain, S. L. Shapiro, S. Swanick, S. C. Roesch, P. J. Mills, I. Bell, G. E. R. Schwartz, A randomized controlled trial of mindfulness meditation versus relaxation training: Effects on distress, positive states of mind, rumination, and distraction. *Ann. Behav. Med.* **33**, 11–21 (2007).

33. J. D. Creswell, A. A. Taren, E. K. Lindsay, C. M. Greco, P. J. Gianaros, A. Fairgrieve, A. L. Marsland, K. W. Brown, B. M. Way, R. K. Rosen, J. L. Ferris, Alterations in resting-state functional connectivity link mindfulness meditation with reduced interleukin-6: A randomized controlled trial. *Biol. Psychiatry* **80**, 53–61 (2016).

34. K. C. R. Fox, M. L. Dixon, S. Nijeboer, M. Girn, J. L. Floman, M. Lifshitz, M. Ellamil, P. Sedlmeier, K. Christoff, Functional neuroanatomy of meditation: A review and meta-analysis of 78 functional neuroimaging investigations. *Neurosci. Biobehav. Rev.* **65**, 208–228 (2016).

35. T. R. A. Kral, T. Imhoff-Smith, D. C. Dean, D. Grupe, N. Adluru, E. Patsenko, J. A. Mumford, R. Goldman, M. A. Rosenkranz, R. J. Davidson, Mindfulness-based stress reduction-related changes in posterior cingulate resting brain connectivity. *Soc. Cogn. Affect. Neurosci.* **14** 777–787 (2019).

36. B. K. Hölzel, J. Carmody, K. C. Evans, E. A. Hoge, J. A. Dusek, L. Morgan, R. K. Pitman, S. W. Lazar, Stress reduction correlates with structural changes in the amygdala. *Soc. Cogn. Affect. Neurosci.* **5**, 11–17 (2010).

37. C. Korponay, D. Dentico, T. R. A. Kral, M. Ly, A. Kruis, K. Davis, R. Goldman, A. Lutz, R. J. Davidson, The effect of mindfulness meditation on impulsivity and its neurobiological correlates in healthy adults. *Sci. Rep.* **9**, 11963 (2019).

38. K. J. Gorgolewski, G. Varoquaux, G. Rivera, Y. Schwarz, S. S. Ghosh, C. Maumet, V. V. Soschat, T. E. Nichols, R. A. Poldrack, J. Poline, T. Yarkoni, D. S. Margulies, NeuroVault.org: A web-based repository for collecting and sharing unthresholded statistical maps of the human brain. *Front. Neuroinform.* **9**, 8 (2015).

39. S. B. Goldberg, J. Wielgosz, C. Dahl, B. Schuyler, D. S. MacCoon, M. Rosenkranz, A. Lutz, C. A. Sebranek, R. J. Davidson, Does the five facet mindfulness questionnaire measure what we think it does? Construct validity evidence from an active controlled randomized clinical trial. *Psychol. Assess.* **8**, 1009–1014 (2015).

40. M. A. Rosenkranz, J. D. Dunne, R. J. Davidson, The next generation of mindfulness-based intervention research: What have we learned and where are we headed? *Curr. Opin. Psychol.* **28**, 179–183 (2019).

41. S. L. Valk, B. C. Bernhardt, F.-M. Trautwein, A. Böckler, P. Kanske, N. Guizard, D. L. Collins, T. Singer, Structural plasticity of the social brain: Differential change after socio-affective and cognitive mental training. *Sci. Adv.* **3**, e1700489 (2017).

42. J. P. Gray, V. I. Müller, S. B. Eickhoff, P. T. Fox Multimodal abnormalities of brain structure and function in major depressive disorder: A meta-analysis of neuroimaging studies. *Am. J. Psychiatry* **177**, 422–434 (2020).

43. L. L. M. Cassiers, B. G. C. Sabbe, L. Schmaal, D. J. Veltman, B. W. J. H. Penninx, F. Van Den Eede, Structural and functional brain abnormalities associated with exposure to different childhood trauma subtypes: A systematic review of neuroimaging findings. *Front. Psychiatry* **9**, 329 (2018).

44. S. Coronado-Montoya, A. W. Levis, L. Kwakkenbos, R. J. Steele, E. H. Turner, B. D. Thombs, Reporting of positive results in randomized controlled trials of mindfulness-based mental health interventions. *PLOS ONE* **11**, e0153220 (2016).

45. A. Hollingshead, *Four Factor Index of Social Status* (Yale University, 1975).

46. D. G. MacCoon, Z. E. Imel, M. A. Rosenkranz, J. G. Sheftel, H. Y. Weng, J. C. Sullivan, K. A. Bonus, C. M. Stoney, T. V. Salomons, R. J. Davidson, A. Lutz, The validation of an active control intervention for Mindfulness Based Stress Reduction (MBSR). *Behav. Res. Ther.* **50**, 3–12 (2012).

47. R. A. Baer, G. T. Smith, E. Lykins, D. Button, J. Krietemeyer, S. Sauer, E. Walsh, D. Duggan, J. M. G. Williams, Construct validity of the five facet mindfulness questionnaire in meditating and nonmeditating samples. *Assessment* **15**, 329–342 (2008).

48. B. Fischl, A. M. Dale, Measuring the thickness of the human cerebral cortex from magnetic resonance images. *Proc. Natl. Acad. Sci.* **97**, 11050–11055 (2000).

49. M. Reuter, N. J. Schmansky, H. D. Rosas, B. Fischl, Within-subject template estimation for unbiased longitudinal image analysis. *Neuroimage* **61**, 1402–1418 (2012).

50. R. S. Desikan, F. Ségonne, B. Fischl, B. T. Quinn, B. C. Dickerson, D. Blacker, R. L. Buckner, A. M. Dale, R. P. Maguire, B. T. Hyman, M. S. Albert, R. J. Killiany, An automated labeling system for subdividing the human cerebral cortex on MRI scans into gyral based regions of interest. *Neuroimage* **31**, 968–980 (2006).

51. D. J. Hagler Jr., A. P. Saygin, M. I. Sereno, Smoothing and cluster thresholding for cortical surface-based group analysis of fMRI data. *Neuroimage* **33**, 1093–1103 (2006).

52. J. A. Maldjian, P. J. Laurienti, R. A. Kraft, J. H. Burdette, An automated method for neuroanatomic and cytoarchitectonic atlas-based interrogation of fMRI data sets. *Neuroimage* **19**, 1233–1239 (2003).

53. N. Tzourio-Mazoyer, B. Landeau, D. Papathanassiou, F. Crivello, O. Etard, N. Delcroix, B. Mazoyer, M. Joliot, Automated anatomical labeling of activations in SPM using a macroscopic anatomical parcellation of the MNI MRI single-subject brain. *Neuroimage* **15**, 273–289 (2002).

54. R Core Team. *R: A Language and Environment for Statistical Computing* (R Foundation for Statistical Computing, 2013).

55. J. Curtin, *lmSupport: Support for Linear Models* (R package version 2.9.13, 2015).

56. I. R. White, N. J. Horton, J. Carpenter, S. J. Pocock, Strategy for intention to treat analysis in randomised trials with missing outcome data. *BMJ* **342**, d40 (2011).

57. S. van Buuren, K. Groothuis-Oudshoorn, MICE: Multivariate imputation by chained equations in R. *J. Stat. Softw.* **45**, 1–67 (2011).

58. D. B. Rubin, *Multiple Imputation for Nonresponse in Surveys* (John Wiley & Sons, 2004).

59. J. Ashburner, K. J. Friston, Voxel-based morphometry—The methods. *Neuroimage* **11**, 805–821 (2000).

60. J. Ashburner, G. R. Ridgway, Symmetric diffeomorphic modeling of longitudinal structural MRI. *Front. Neurosci.* **6**, 197 (2013).

61. C. Gaser, R. Dahnke, CAT - A computational anatomy toolbox for the analysis of structural MRI data. *HBM* **2016**, 336–348 (2016).